10

Functionalized Graphene Sheet / Polyurethane Nanocomposites

Hyung-il Lee and Han Mo Jeong
Department of Chemistry, University of Ulsan, Ulsan 680-749, Republic of Korea

1. Introduction

One of an integral aspect of polymer nanotechnology is precise synthesis of polymer nanocomposites. [1-6] Small insertion of nanosized inorganic compounds usually improves the properties of polymers in a great deal, which makes many of the most important application areas possible depending on the inorganic material present in polymers. [7] Specially, polymer composites which contain electrically conducting inorganic fillers, such as natural graphite, carbon black and metal powders, have been extensively investigated in the past few decades for their potential applications in antistatic coatings, electromagnetic shielding and corrosion-resistant coatings, etc. [8-10] Sometimes, in order to obtain an electrical conductivity of 10^{-4} S cm^{-1} required for commercial uses, these composites often contain as much as 15 wt% filler, which in turn causes deterioration of mechanical properties and poor processability. It is, therefore, important to use a small amount of filler to retain the stretchability or transparency of a matrix polymer.

Graphene is essentially an isolated atomic plane of graphite, which is composed of a single layer sheet of sp^2-bonded carbon atoms that are densely packed in a honeycomb crystal lattice with large specific surface area. [11,12] Single-layer graphene sheet have been of great interest for their unique properties, including not only excellent mechanical properties but thermal conductivity and stiffness. Given these unique properties, graphene has been considered as an ideal reinforcing agent for high strength polymer composites. [13,14] In addition, the elusive two-dimensional structure of graphene has a number of unusual electronic and robust transport properties that may be useful in the electronics or in the related regions. [15-17]

The properties of polymer nanocomposites depend strongly on how well inorganic fillers are dispersed in the polymer matrix. A great deal of nanocomposite research using carbon nanotubes (CNT) as nanosize conductive fillers has focused on finding better methods for dispersing nanotubes into polymers since pristine carbon nanotubes have poor compatibility with most organic solvents and polymers. For this reason, additional surface treatment is necessary for CNT based nanocomposites to allow better compatibility. [18] Though surface modification via acid modification and polymer grafting improves solubility of CNT in solvents and polymers somehow, the extent of disentanglement of the CNT bundles into polymers is low, and severe sonication often leads to disruption of the CNT. In case of graphene, during the synthesis of graphene from graphite oxide (GO)[19] some epoxide and hydroxyl groups remain, which greatly facilitate dispersion. [20] There

could be minor issues related to restacking of the flat graphene sheets after chemical or thermal reduction, which might decrease dispersion efficiency. However, small addition of surfactants can efficiently prevent individual graphene sheets from restacking with each other by stabilizing the reduced particle suspensions. By virtue of these benefits, it is considered that graphene-based nanocomposites have better performance than their CNT-based counterparts.

While composites with graphene have been prepared with a number of polymers, polyurethane (PU) was one of the mostly studied polymers [21]. PU can provide properties covering from a high performance elastomer to tough thermoplastic with excellent physical properties, including high tensile strength, abrasion and tear resistance, and solvent resistance. In addition, high versatility in chemical structures originated from a wide range of monomeric materials affords tailor-made properties with well-designed combinations of these monomers. As a result, PU can be easily manipulated to satisfy the highly diversified demands of modern technologies.

Driven by modern requirements to decrease emissions of volatile organic compounds, the development of environmentally friendly waterborne polyurethane (WPU) has been increasing, especially in the field of coating industry where the reduction of evolution of volatile organic compounds during the drying process is critical. [22-24] In addition, WPU offers many advantages such as low viscosity at high molecular weight and good applicability, which cannot be realized with conventional solvent-borne systems. They could be also utilized effectively in electronic devices as coatings for antistatic or electromagnetic shielding if they could be modified for improved conductivity. This can be achieved with nanosize conductive fillers that can possibly make a percolative network at an extremely low loading. [25]

The first area covered will pertain to general preparation of graphite oxide (GO) and functionalized graphene sheets (FGS) with a focus on methods suitable for polymer composite applications. Several examples of graphene-based nanocomposites with various polymers are also discussed. Secondly, the preparation and physical properties of functionalized graphene sheet (FGS)/PU nanocomposites are highlighted.

2. Preparation of FGS

Graphenes can be made by two methods; bottom-up and top-down. Chemical vapor deposition (CVD)[26], arc discharge[27], and epitaxial growth on SiC[28] are usually employed to synthesize graphenes in the bottom-up approaches. In most cases, a variety of graphene preparations rely on the top-down approaches that utilize a cheap and commercially available graphite as a starting material. In this section, the top-down approaches are focused.

Synthetically, a variety of top-down approaches have been adopted to allow the preparation of graphenes. Generally, there are three methods for the synthesis of graphenes: “direct exfoliation of graphite”, “chemical reduction of GO”, and “thermal reduction of GO”. The “direct exfoliation of graphite” route involves micromechanical cleavage of graphite. This method allows graphenes with large-size and high-quality. It is difficult, however, to separate the exfoliated graphene sheets from the bulk graphite. In the “chemical reduction of GO” method, the starting material is graphite oxide (GO) produced by oxidation of graphite. GO is not completely exfoliated and contain extensive domains of stacked graphitic layers. The resulting GO is dispersed in solvent and chemically reduced to graphene sheets by reducing agents such as hydrazine, dimethylhydrazine, hydroquinone,

etc. "Thermal reduction of GO" strategy also begins with the preparation of GO. It is generally believed that each layer of GO consists of randomly distributed unoxidized aromatic regions and six-member aliphatic regions with polar groups, such as hydroxyl, epoxide, ether, and carboxylate groups, originated from oxidation. When a sufficiently oxidized GO is heated in an inert environment over 1000 ^{o}C, it can be exfoliated into a few layered graphene sheets, that is, functionalized graphene sheets (FGSs). This step accompanies pressure build-up which stems from CO_2 evolution due to the decomposition of the epoxy and hydroxyl groups that bridges each GO sheet. [29-31] As a result, an exfoliated GO, in which the inter-graphene spacing associated with GO and the graphite is almost completely excluded after thermal expansion, has an affinity for polar solvents and polymers, as well as good conductivity. These properties stem from the fact that the completely exfoliated GO is composed of a few layered FGSs that still contain the polar functional groups that remain after thermal treatment.[32] In addition, from the industrial point of view, this method is preferred since large scale bulk production of FGS is possible.
In this chapter, we confine our focus to thermally exfoliated FGSs since polymer/graphene composites that we will discuss are based on them. The following section coverd will briefly survey various types of polymers that have been used for nanocomposites with graphenes. Among them, poly(methyl methacrylate) (PMMA)/graphene nanocomposites are focused.

3. PMMA/graphene nanocomposites

Generally, FGS-based polymer composites benefit their excellent performance from graphene's thermal, mechanical and electrical properties. These composites are electrically conducting and have higher thermal stability than polymer alone. In addition, incorporation of a small amount of graphene into polymer matrix offers a great opportunity to make tough and lightweight materials as long as graphenes are homogeneously distributed in polymer matrices. There have been numerous reports on preparation of polymer/graphene nanocomposites with different kinds of polymer materials, including polystyrene (PS)[33], polycarbonate (PC)[34], PMMA[35-37], and PU.[38,39]

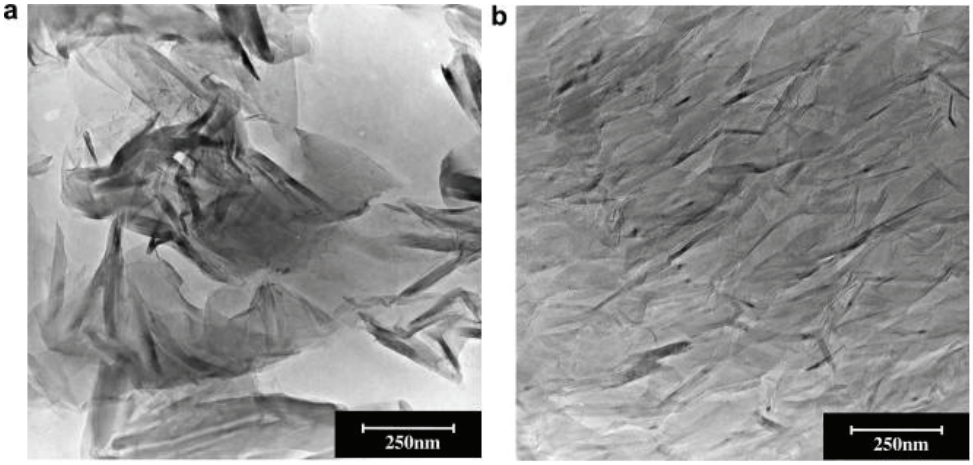

Fig. 1. TEM micrographs of PMMA/GO nanocomposites: (a) a PMMA/GO composite with 6.7 parts of GO, (b) a PEO-PMMA multi-block copolymer/GO composite with 6.7 parts of GO. Adapted with permission from Ref. [36]. Copyright 2005 Elsevier Ltd.

In our group, we began to examine PMMA as a matrix polymer material in which GO or FGS were incorporated. In the first study, PMMA/GO nanocomposites were prepared by in situ polymerization of methyl methacrylate (MMA) in the presence of GO. A the macroazoinitiator (MAI) containing a poly(ethylene oxide) (PEO) segment that was employed for this polymerization, was intercalated between the lamellae of GO to induce the inter-gallery polymerization of MMA and exfoliate the GO.[36] The morphological, conductivity, thermal, mechanical and rheological properties of these nanocomposites were examined and compared with those of intercalated nanocomposites prepared by polymerization with the normal radical initiator, 2,2'-azobisisobutyronitrile. Since it has been reported that PEO can be easily intercalated at the GO gallery[40,41], it is expected that the polymerized PEO-PMMA multi-block copolymer will have an affinity to GO due to the presence of PEO block, which cannot be easily achieved with a composite prepared by a conventional small molecular weight initiator. As shown in Fig 1, PEO-PMMA multi-block copolymer/GO composites have the finer dispersion than PMMA/GO composites due to PEO being easily intercalated at the GO gallery. It was also evident that conductivity of PEO-PMMA multi-block copolymer/GO composites was increased compared to that of PMMA/GO composites. For example, a conductivity of 1.78×10^{-7} S/cm was attained in the exfoliated PEO-PMMA multi-block copolymer/GO composites prepared with 2.5 parts GO per 100 parts MMA, which was about 50-fold higher than that of intercalated PMMA/GO composites.

Secondly, compatibilizing effect of GO in PMMA/FGS nanocomposites has been investigated.[37] While we have prepared and examined FGS nanocomposites with various polymers, it was found that the dispersability of FGS in a polymer matrix can be improved when GO was used as a compatibilizer. The compatibilizing effect of GO is originated from its chemical resemblance to FGS as well as polar functional groups that can interact with matrix PMMA. An PMMA/FGS nanocomposite containing 1 part FGS has a conductivity of 1.89×10^{-7} S/cm, more than 10^{7}-fold better than pristine PMMA. This conductivity was enhanced a further 100-fold by addition of 1 part GO. These results were ascribed to compatibilizing ability of GO to allow the fine dispersion of FGS in a PMMA matrix.

4. PU/FGS nanocomposites

Generally, PU/graphene nanocomposites can be prepared by two methods: "mechanical mixing method" and "in situ polymerization method". The "mechanical mixing method" includes solvent and melt process. Solvent process is usually used such that graphenes were mixed with a PU matrix via blending with solvents followed by solvent removal. It is often advantageous to employ "mechanical mixing" approach that can offer simple and facile preparation of nanocomposites. It is, however, less efficient to achieve uniform dispersion of graphenes in a polymer matrix. "In situ polymerization method" involves intercalative polymerization of monomers in the presence of graphenes. It is considered that it is a better approach for dispersing graphenes into polymers. However, this approach is limited to solvent process due to the high viscosity of even dilute dispersion of graphene.

4.1 Preparation of FGS/PU nanocomposites.

As discussed briefly in the previous section, various types of graphene-based polymer composites have been investigated. Extensive literature on graphene-based polymer composites is beyond the scope of discussion in this chapter. The representative examples

illustrating approaches to preparing FGS/PU nanocomposites are presented. Different aspects of FGS/PU nanocomposites, including electrical conductivities, thermal properties, and mechanical properties, will be thoroughly discussed based on our published results. As mentioned above, FGSs that were used to prepare PU/graphene composites were thermally exfoliated. Two different types of PU, organic solvent borne TPU and WPU, were employed to make four different kinds of nanocomposites with combination with two different processing methods, mechanical mixing and in situ polymerization.

1. FGS/organic solvent borne TPU nanocomposites prepared by mechanical mixing (TPUN).[42]
2. FGS/organic solvent borne TPU nanocomposites prepared by in situ polymerization (TPUNC).[43]
3. FGS/water-borne PU nanocomposites prepared by mechanical mixing (WPUN).[44]
4. FGS/water-borne PU nanocomposites prepared by in situ polymerization (WPUCL, WPUMG).[21]

4.1.1 FGS/organic solvent borne TPU nanocomposites prepared by mechanical mixing (TPUN)

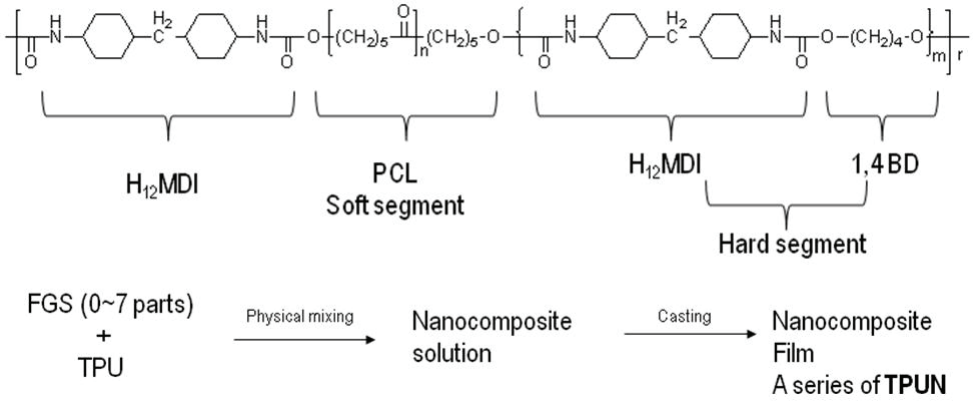

Fig. 2. A chemical structure of TPU (Up) and the preparation of nanocomposite films by a mechanical method (Down).

Fig 2 shows the structure of TPU that was used in this work. TPU/FGS nanocomposite solution was obtained by mixing different amounts of FGS in the presence of TPU in methylethylketone (MEK). Sample designation codes provide information regarding the amount of FGS included in the TPU samples. For example, TPUN-5 contains 5 parts of FGS per 100 parts of polymer.

4.1.2 FGS/organic solvent borne TPU nanocomposites prepared by in situ polymerization (TPUNC)

To prepare the TPU/FGS nanocomposite by the in situ polymerization method, the FGS was immersed in MEK where polymerization was performed (Fig 3). The TPU/FGS nanocomposites were prepared by using 0 to 3 parts of FGS per 100 parts TPU since flexible cast films were unachievable when the content of FGS was more than 3 parts per 100.

Sample designation codes were given by the amount of FGS included in the TPU samples. For example, TPUNC-3 contains 3 parts FGS per 100 parts TPU.

Fig. 3. The preparation of FGS/TPU nanocomposite films by in situ polymerization method.

4.1.3 FGS/water-borne PU nanocomposites prepared by mechanical mixing (WPUN)

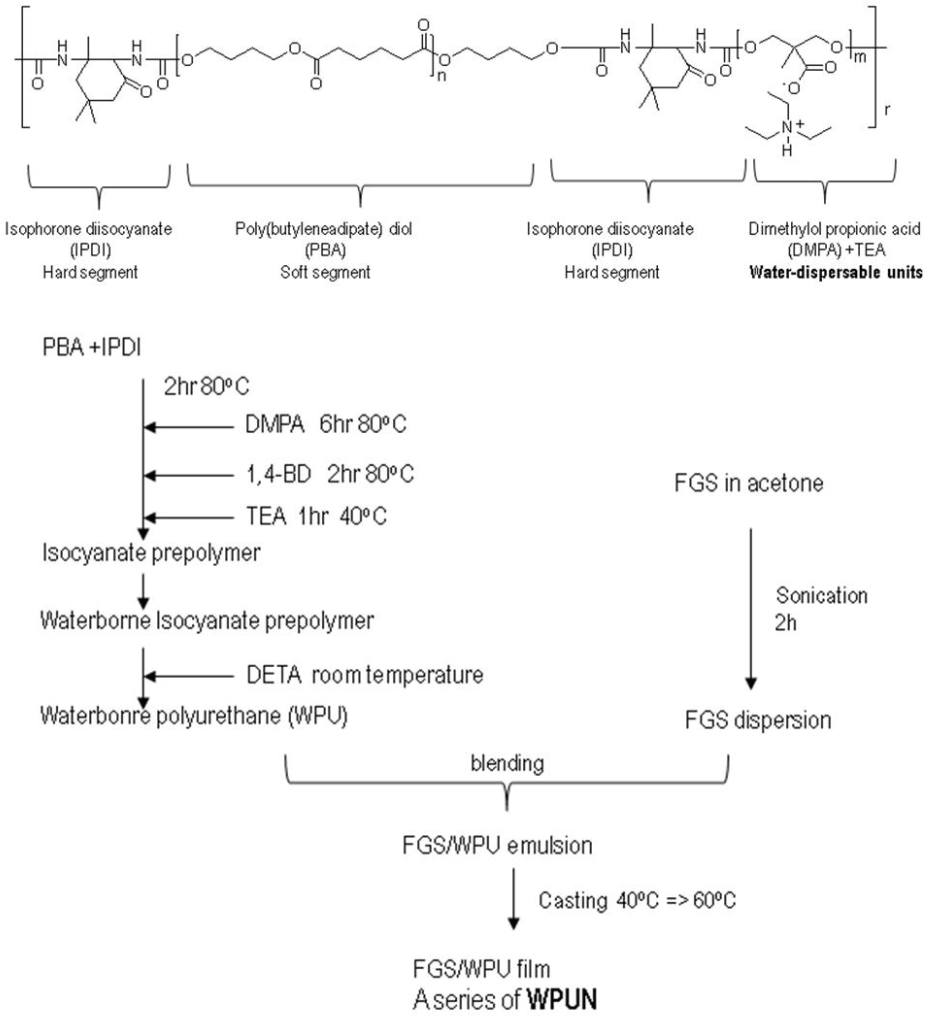

Fig. 4. A chemical structure of WPU (Up) and the preparation of nanocomposite films by a mechanical method (Down).

As schematically presented in Fig 4, the structure of WPU includes water-dispersable units (salt of DMPA and TEA). WPU/FGS nanocomposite solution was obtained by mixing different amount of FGSs (0 to 6 parts) in acetone with WPU in water. Sample designation codes were given by the amount of FGS included in the TPU samples. For example, WPUN-5 contains 5 parts of FGS per 100 parts of WPU.

4.1.4 FGS/water-borne PU nanocomposites prepared by in situ polymerization (WPUCL, WPUMG)

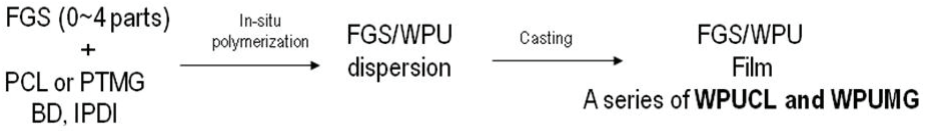

Fig. 5. The preparation of FGS/WPU nanocomposite films by in situ polymerization method.

Basically, the structure of WPU is the same as one that used in mixing method except that poly(tetramethylene glycol) (PTMG) was used along with PCL as a soft segment. FGS/WPU nanocomposites were made by in situ polymerization in the presence of FGS (Fig 5). Sample designation codes were given by the amount of FGS included in the WPU samples. For example, WPUCL-2 and WPUMG-2 contain 2 parts of FGS per 100 parts of WPU based on PCL and PTMG, respectively, as a soft segment.

4.2 Characterization of FGS/PU nanocomposites.

Characterization of successful preparation of FGS/PU nanocomposites rely on a variety of instruments such as transmission electron microscopy (TEM), FT-IR, and XRD. It is often difficult to characterize FGS/PU nanocomposites quantitatively by TEM due to wrinkled nature and small thickness of graphenes. Nonetheless, TEM has been one of the most widely used imaging techniques to visualize layered structures of graphenes. As shown in Fig 6, FGSs are finely dispersed in the PU matrices with subnano-sized thicknesses and high aspect ratios, demonstrating the good compatibility between the FGS and TPU. According to these images that show well dispersion of FGS, it is expected that effective conductive channels can be created for all cases of FGS/PU nanocomposites.

Figure 7 shows the wide-angle XRD patterns of the graphite, GO and FGS specimens. The diffractogram of graphite shows a very intense and narrow peak at 2θ = 26.5°, which corresponds to the X-ray reflection on the (002) planes of well-ordered graphenes with interlayer spacing, I_c, between the well ordered graphenes being 3.35 Å. GO has a broad peak at 2θ = 14.1° due to I_c being expanded to 6.27 Å by the accommodation of various functional groups on the graphene surface. However, FGS has no visible peak at the range of $2\theta > 2°$, which indicates the notable expansion and sufficient disorder of the graphene layers.

It is also possible to characterize FGS/PU nanocomposites with XRD patterns. Generally, one can attain very important information from XRD patterns of nanocpmposites: "extent of dispersion of FGS in a polymer matrix", which can be evaluated in two ways. Firstly, whether or not there exist visible peaks at the range of $2\theta > 2°$ due to long range order of the stacked FGSs. Secondly, whether or not peaks of crystalline segments of PU decrease upon

increased addition of FGSs. For example, the dispersed FGS does not give rise to any new wide-angle XRD peak at the range of $2\theta > 2^{\circ}$ (Fig 8). This suggests that either (1) the distance between the FGSs is far enough or (2) no long-range order exists even when the FGS has a stacked structure. Fig 8 also shows that the diffractogram of TPUN-0, which doesn't contain FGSs, has two peaks at $2\theta = 21.1^{\circ}$ and 23.3°. These peaks are attributed to the reflections on the (110) plane and the (200) plane of the PCL crystal, respectively. The intensity of these peaks decreases as the content of FGS increased due to the frustrated crystallization of the PCL phase by increasing amounts of FGS.

Sample codes		Tensile properties			Conductivity (S/cm)
		Modulus (MPa)	Tensile strength (MPa)	Elongation at break (%)	
TPUN	TPUN-0	458±23	20.0±0.1	814±64	4.58×10^{-11}
	TPUN-0.5	559±113	18.8±0.1	779±40	8.37×10^{-11}
	TPUN-1	557±85	17.8±0.3	693±34	4.62×10^{-10}
	TPUN-2	639±70	13.4±0.1	686±43	5.41×10^{-4}
	TPUN-3	657±157	15.5±0.3	693±52	5.88×10^{-4}
	TPUN-4	636±47	17.0±0.1	517±13	8.54×10^{-4}
	TPUN-5	351±2	18.8±0.9	347±73	9.16×10^{-4}
	TPUN-7	357±43	18.9±0.2	245±22	4.92×10^{-4}
TPUNC	TPUNC-0	59±19	7.4±0.5	1368±55	2.85×10^{-11}
	TPUNC-1	138±5	4.3±0.4	898±7	6.81×10^{-10}
	TPUNC-2	150±28	4.8±0.4	653±73	2.07×10^{-3}
	TPUNC-3	171±9	3.7±0.4	428±15	2.77×10^{-3}
WPUN	WPUN-0	66.2±9.0	29.6±0.9	478±44	1.34×10^{-10}
	WPUN-0.5	38.9±7.6	35.8±8.8	551±185	1.57×10^{-10}
	WPUN-1	54.7±6.1	40.0±4.6	590±88	1.90×10^{-10}
	WPUN-2	55.9±4.8	36.2±1.0	457±43	1.31×10^{-5}
	WPUN-3	53.6±11.5	32.5±3.3	458±83	2.24×10^{-4}
	WPUN-4	48.1±13.1	38.9±8.3	452±110	2.53×10^{-4}
	WPUN-5	56.9±3.8	31.2±6.4	402±97	5.47×10^{-4}
	WPUN-6	72.9±2.5	26.2±2.2	290±1	2.75×10^{-4}
WPUCL	WPUCL-0	79.6±4.9	21.6±6.8	553±91	8.84×10^{-11}
	WPUCL-1	87.5±20.9	11.9±4.3	448±77	4.14×10^{-11}
	WPUCL-2	99.9±15.6	7.5±0.4	415±19	7.03×10^{-10}
	WPUCL-3	115.2±23.7	7.1±0.6	374±26	1.20×10^{-5}
	WPUCL-4	345.5±102.2	5.9±4.8	46±10	7.87×10^{-4}
WPUMG	WPUMG-0	80.5±9.1	27.9±7.3	638±61	1.68×10^{-11}
	WPUMG-1	85.8±2.9	20.9±3.0	688±38	2.00×10^{-11}
	WPUMG-2	93.8±17.0	13.4±0.3	586±40	2.76×10^{-10}
	WPUMG-3	1009.9±9.7	7.4±1.5	409±117	3.17×10^{-4}
	WPUMG-4	145.5±7.0	5.1±0.6	151±32	1.91×10^{-3}

Table 1. Physical properties of PU/FGS nanocomposites.

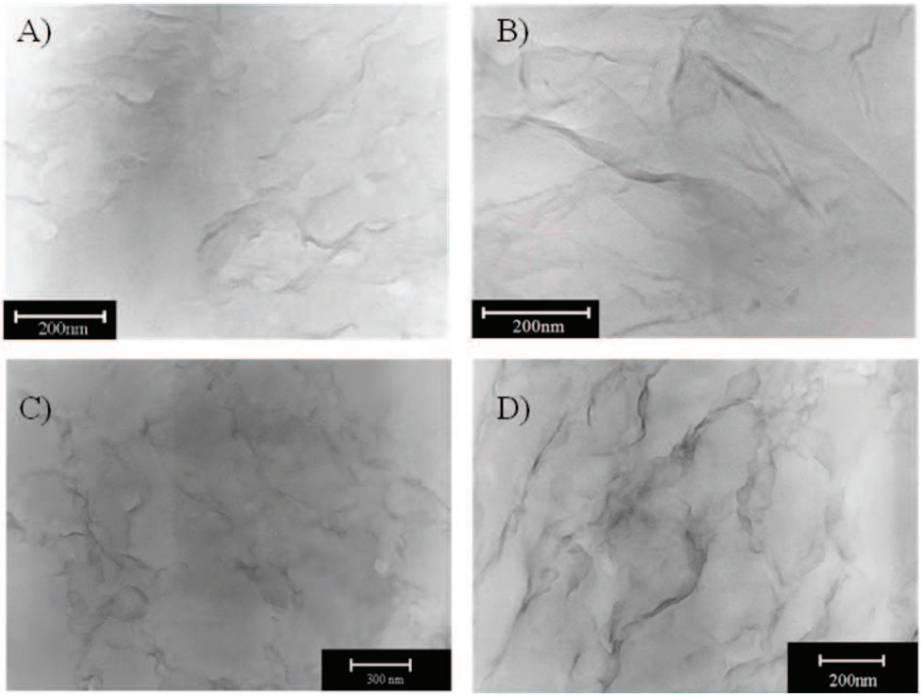

Fig. 6. TEM micrographs of FGS/PU nanocomposites: (A) TPUN-4, (B) TPUNC-3, (C) WPUN-3, (D) WPUCL-4. Adapted with permission from Ref. [42] and [21]. Copyright 2009 Wiley-VCH Verlag GmbH & Co. KGaA.

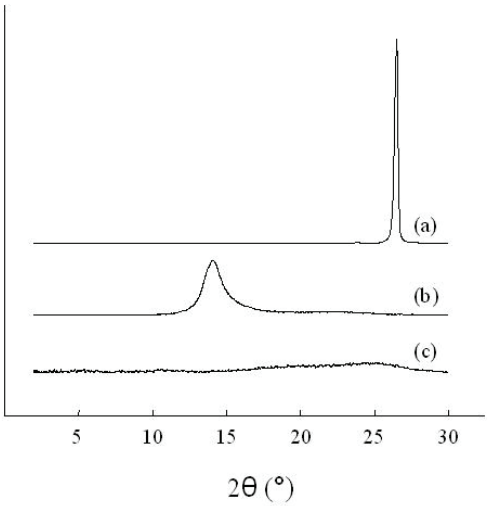

Fig. 7. XRD patterns of graphite, GO, and FGS. Adapted with permission from Ref. [42]. Copyright 2009 Wiley-VCH Verlag GmbH & Co. KGaA.

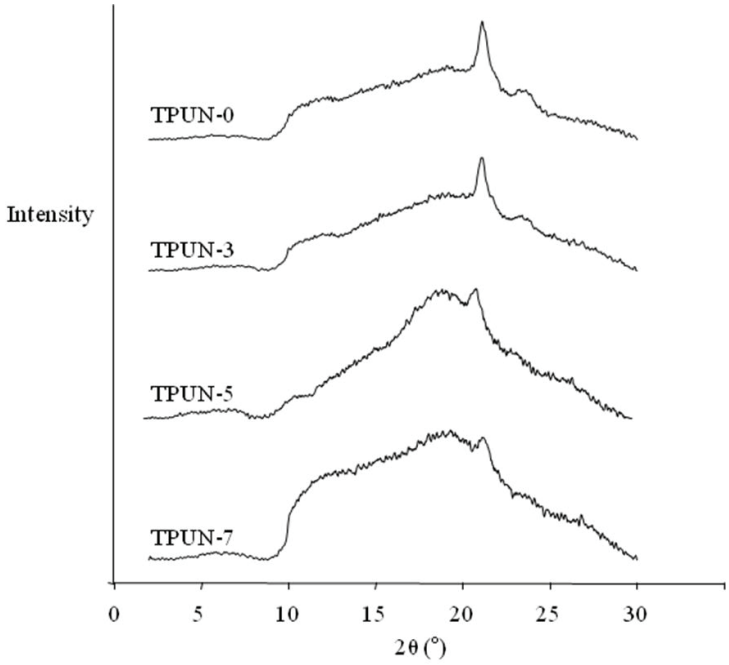

Fig. 8. XRD patterns of a series of TPUN. Adapted with permission from Ref. [42]. Copyright 2009 Wiley-VCH Verlag GmbH & Co. KGaA.

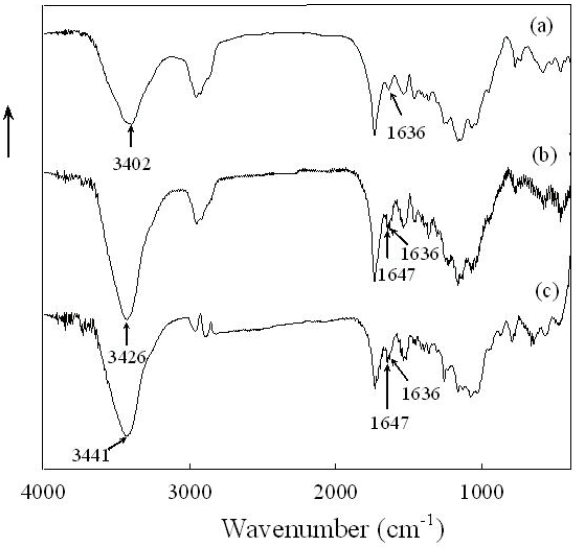

Fig. 9. FTIR spectra of (a) WPUN-0, (b) WPUN-3, and WPUN-6. Adapted with permission from Ref. [44]. Copyright 2008 Wiley-VCH Verlag GmbH & Co. KGaA.

FT-IR is another important tool to evaluate even dispersion of FGSs in a PU matrix. Specifically, by monitoring the intensity of hydrogenbonded N-H absorption band of urethane linkage, one can have an idea on the extent of dispersion of FGS. For example, the N–H stretching vibration of polyurethane in the range of 3,300~3,600 cm^{-1} is highly sensitive to hydrogen bond distribution. Absorption bands of hydrogenbonded and free N–H are located at 3,330 and 3,400 cm^{-1}, respectively. WPUN-0 (pristine WPU without addition of FGSs) has an absorption band at 3,402 cm^{-1}, which moves to a higher wavenumber with increased FGS content (Fig 9). This demonstrates that the high contents of FGSs weakened the interaction of hydrogen bonding between urethane linkages.
Overall, it is concluded that the extent of dispersion of FGSs in a PU matrix can be effectively evaluated by TEM, XRD, and FT-IR. In the following section, we discuss thermal properties of FGS/PU nanocomposites.

4.3 Thermal properties of FGS/PU nanocomposites.

Number of washing	Residue (wt%)	
	Physical mixing method	*In situ* polymerization method
1	32.7	26.5
2	38.7	33.9
3	43.4	37.3
6	46.5	39.3
9	50.3	41.1

Table 2. Residual weights of washed FGS after thermal degradation.[43]

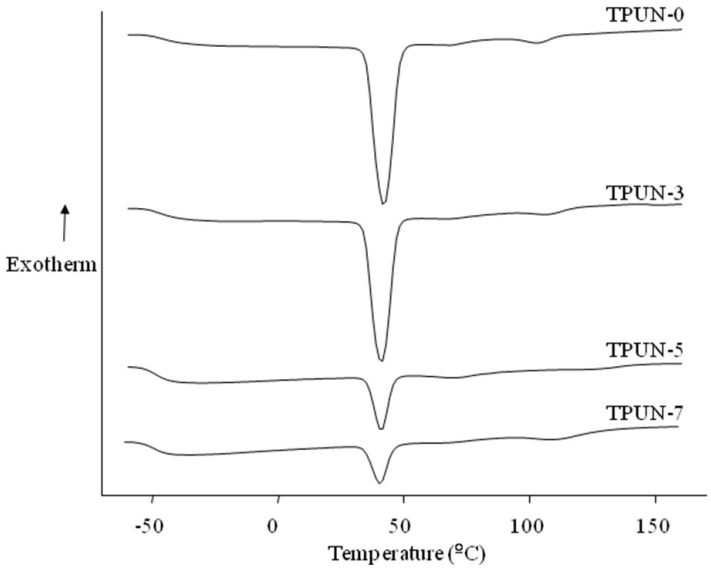

Fig. 10. DSC thermograms of a series of TPUN. Adapted with permission from Ref. [42]. Copyright 2009 Wiley-VCH Verlag GmbH & Co. KGaA.

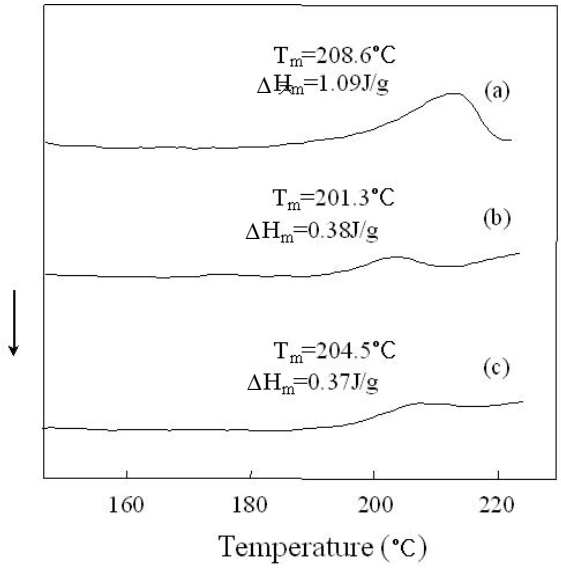

Fig. 11. DSC thermograms obtaind on heating of (a) WPUN-0, (b) WPUN-3, and (c) WPUN-6. Adapted with permission from Ref. [44]. Copyright 2008 Wiley-VCH Verlag GmbH & Co. KGaA.

As with the above three characterization tools, DSC and TGA can also provide useful information on how well FGSs are distributed in a PU matrix. Both TPU and WPU that were employed for the preparation of nanocomposites have soft and hard crystalline segments. By observing changes of glass transition temperature (T_g), crystalline melting temperature, and heat of fusion of each crystalline domain that are induced by added FGSs, one can assess how thermal properties are affected by addition of FGSs. For example, for a series of TPUNC prepared by in situ polymerization, the chemical and/or physical interactions between FGS and TPU were enhanced, as compared to a series of TPUN prepared by the physical mixing method. That is, gravimetry showed that the amount of TPU adhered onto FGSs increased when the nanocomposite was prepared by the in situ polymerization method (Table 2).[43] From the DSC thermogram of TPUN-0, one can see a sharp melting endothermic peak of the soft segment (T_{ms}) and a small endothermic melting peak of the hard segment (T_{mh}) at 41.8 and 103.2 ^{o}C, respectively (Fig 10). As the amount of FGS in the nanocomposites increased, the heat of fusion at T_{ms} (ΔH_{ms}) decreased and dropped abruptly at higher contents of FGS. This suggests that the crystallization of the PCL segment is inhibited by the FGS, more evidently at higher contents of FGS. This decrease in the crystallinity also seems to cause a decrease in T_g with increasing contents of FGS. Similar behaviors were observed for a series of WPUN systems in which melting of hard segments is more evident than that of soft segments (Fig 11). The melting endothermic peak (T_m) 200 ^{o}C and the heat of fusion (ΔH_m) of the hard segment decreased as contents of FGS increased, indicating that the crystallization of the hard segment was inhibited by FGSs.

4.4 Mechanical properties of FGS/PU nanocomposites.

Graphene is the one of the stiffest material with high intrinsic strength. When it is used as a filler, it is expected that a reinforced composite can have superior mechanical properties.

Moreover, one can further increase mechanical properties of the composite by employing different processing techniques. Here, we compare two processing methods, mechanical mixing and in situ polymerization, in detail and how mechanical properties of the resulting composites are affected by how they were made. As shown in Table 1, tensile modulus was enhanced with increasing amount of FGS for the series of TPUN and TPUNC. However, tensile strength and elongation at break gradually decreased with increase of the content of FGS, which is due to inhibition of molecular rearrangement and orientation with respect to the tensile axis during deformation. The reduced crystallinity of the soft segment can also contribute to these reductions of tensile strength and elongation at break. For the cases of TPUN and TPUNC, if TPUs are highly elongated, hard segments break apart when phase mixed with soft segments; the hard and soft segments orient in the direction of elongation, resulting in maximum intermolecular interaction. The evident lowering of tensile properties measured at large deformation suggested that these molecular rearrangements were interrupted in the presence of FGSs. This behavior became more evident for a series of TPUNC. When TPU was physically mixed with 3 parts of FGS (TPUN-3), the increase of modulus and the decrease of tensile strength and elongation at break were 43%, 23%, and 15%, respectively, of that of TPUN-0. In contrast, these respective changes, compared to TPUNC-0, are 190%, 50%, and 69% in the nanocomposites made by the in situ polymerization method (TPUNC-3). These results suggest that the interactions between FGS and TPU increased when prepared by the in situ polymerization method, and that the increased interactions reduce the chain mobility for realignment.

For the series of WPUCL and WPUMG, one can see that the modulus of WPU is effectively improved by the addition of FGS. For a series of WPUN, which were prepared by a simple physical mixing method, modulus decreased by the addition of FGSs. The interactions between hard segments were suppressed by the presence of FGSs, which overwhelmed the reinforcing effect of FGS. For the series of WPUCL, however, the reinforcing effect of FGS itself and the increased crystallinity of the soft segment in the presence of FGS overshadowed the effect on the modulus of decreased interactions between hard segments by FGSs. The interaction between the FGS and WPU molecules are stronger in the nanocomposites prepared by the in situ method than those made by a simple mixing method, and this consequently enhanced the reinforcing effect of FGS.

Overall, performance of FGS as s mechanical reinforcement material is as competitive as over existing carbon fillers such as carbon black and CNT. For all of FGS/PU composites, enhancement of modulus with better graphene dispersion is clearly demonstrated. Tensile strength and elongation at break dropped significantly with the addition of rigid fillers. In addition, modulus is greatly influenced by the interaction between FGS and PU. The modulus improvement of FGS/PU composites made by in situ polymerization is more evident than those made by a physical mixing method, supporting our reasoning that the interaction between FGS and WPU gets stronger when made by an in situ polymerization method.

4.5 Electrical conductivities of FGS/PU nanocomposites.

Due to conjugated nature of flat graphene sheets, the composites are electrically conductive through percolated channels generated for electron transfer. Moreover, graphene-based nanocomposites have very low percolation threshold, which allows the efficient preparation of the nanocomposite with high electrical conductivity at significantly low loading. The

extent of graphene dispersion can be estimated by the onset concentration for electrical percolation. For example, in case of TPUN-2, the 2 part addition of FGSs improved electrical conductivity by 10^7 times compared with TPUN-0 (Table 1). Evenly distributed FGSs with nano-sized thicknesses and high aspect ratios (Figure 6) can create an effective conductive channel. For the same amount of FGS loading, the conductivities of a series of TPUNC made by in situ polymerization method is slightly higher than those of a series of TPUN made by physical mixing, indicating that the dispersion of FGS in a TPU matrix is improved by in situ polymerization method (Fig 12).

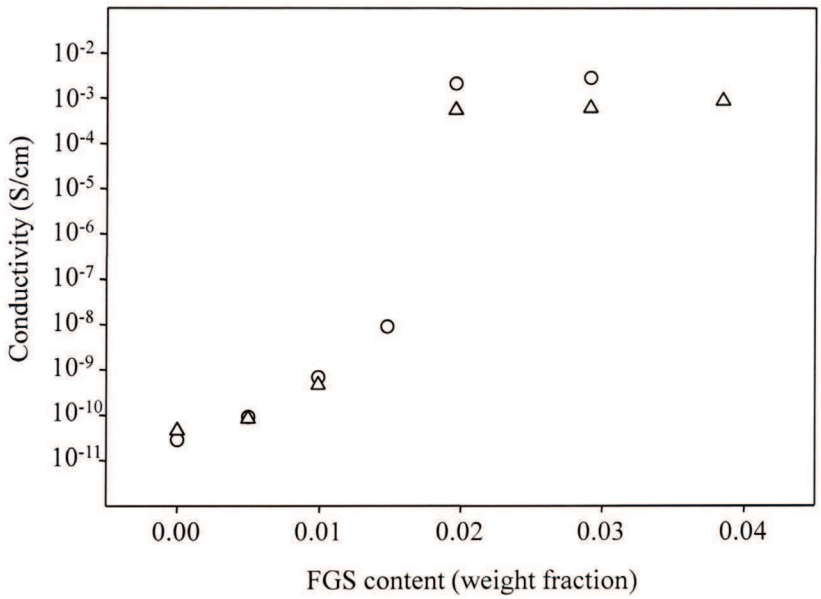

Fig. 12. Conductivities of TPU/FGS nanocomposites made by the in situ polymerization method (○) and by the physical mixing method (Δ)[43]

When preparing a series of WPUN, emulsion stability should be considered since high loading of FGSs might cause FGS/WPU emulsion unstable. Therefore, sufficiently high electrical conductivity and enough emulsion stability must be balanced for successful nanocomposite films. As expected, the conductivity of WPU increased drastically by the addition of FGS. The addition of two parts FGS per 100 parts of WPU (WPUN-2) led to about a 10^5-fold increase in conductivity. However, the conductivity of nanocomposite did not rise evidently above WPUN-3 while the emulsion stability decreased with increasing contents of FGS. WPUN-3 was optimal for the commercial production of WPU/FGS nanocomposites with excellent balance between electrical conductivity and emulsion stability.

5. Conclusions

With benefits arising from a variety of excellent properties of the FGS, FGS-based novel nanocomposites are constantly being developed. Especially, FGS/PU nanocpmposites

covered here exhibit excellent thermal, mechanical, and electrical properties. These properties can significantly vary with a processing method which determines the extent of dispersion and interaction of FGSs with PU matrices. We compared two processing methods, mechanical mixing and in situ polymerization, in detail and how properties of the resulting composites are affected by how they were made. It was observed that the modulus improvement by the reinforcing effect of FGS and high electrical conductivities were more evident when the nanocomposites of WPU with FGS were prepared by an in situ method, which suggested that the interaction between FGS and PU was stronger when made by an in situ method.

6. Acknowledgement

This work was supported by Priority Research Centers Program through the National Research Foundation of Korea (NRF) funded by the Ministry of Education, Science and Technology (2009-0093818).

7. References

[1] Du, M.; Guo, B.; Jia, D. *Polym. Int.* 2010, *59*, 574-582.
[2] Kiliaris, P.; Papaspyrides, C. D. *Prog. Polym. Sci.* 2010, *35*, 902-958.
[3] Sahoo, N. G.; Rana, S.; Cho, J. W.; Li, L.; Chan, S. H. *Prog. Polym. Sci.* 2010, *35*, 837-867.
[4] Shanmuganathan, K.; Capadona, J. R.; Rowan, S. J.; Weder, C. *Prog. Polym. Sci.* 2010, *35*, 212-222.
[5] Spitalsky, Z.; Tasis, D.; Papagelis, K.; Galiotis, C. *Prog. Polym. Sci.* 2010, *35*, 357-401.
[6] Djokovic, V.; Radhakrishnan, T.; Nair, P. S.; Comor, M. I.; Nedeljkovic, J. M. *Recent Adv. Polym. Nanocompos.* 2009, 227-268.
[7] Osman, M. A.; Mittal, V.; Suter, U. W. *Macromol. Chem. Phys.* 2007, *208*, 68-75.
[8] Kalaitzidou, K.; Fukushima, H.; Drzal, L. T. *Compos. Sci. Technol.* 2007, *67*, 2045-2051.
[9] Li, J.; Sham, M. L.; Kim, J.-K.; Marom, G. *Compos. Sci. Technol.* 2007, *67*, 296-305.
[10] Sandler, J. K. W.; Kirk, J. E.; Kinloch, I. A.; Shaffer, M. S. P.; Windle, A. H. *Polymer* 2003, *44*, 5893-5899.
[11] Kim, H.; Abdala, A.; Macosko, C. W. *Macromolecules* 2010, *43*, 6515-6530.
[12] Kim, J.; Kim, F.; Huang, J. *Mater. Today* 2010, *13*, 28-38.
[13] Fang, M.; Wang, K.; Lu, H.; Yang, Y.; Nutt, S. *J. Mater. Chem.* 2009, *19*, 7098-7105.
[14] Vickery, J. L.; Patil, A. J.; Mann, S. *Adv. Mater.* 2009, *21*, 2180-2184.
[15] Zhang, H.; Bao, Q.; Tang, D.; Zhao, L.; Loh, K. *Appl. Phys. Lett.* 2009, *95*, 141103/1-141103/3.
[16] Bao, Q.; Zhang, H.; Yang, J.-x.; Wang, S.; Tang, D. Y.; Jose, R.; Ramakrishna, S.; Lim, C. T.; Loh, K. P. *Adv. Funct. Mater.* 2010, *20*, 782-791.
[17] Liu, J.; Tao, L.; Yang, W.; Li, D.; Boyer, C.; Wuhrer, R.; Braet, F.; Davis, T. P. *Langmuir* 2010, *26*, 10068-10075.
[18] Chen, J.; Liu, H.; Weimer, W. A.; Halls, M. D.; Waldeck, D. H.; Walker, G. C. *J. Am. Chem. Soc.* 2002, *124*, 9034-9035.
[19] Dreyer, D. R.; Park, S.; Bielawski, C. W.; Ruoff, R. S. *Chem. Soc. Rev.* 2010, *39*, 228-240.
[20] Wiemann, K.; Kaminsky, W.; Gojny, F. H.; Schulte, K. *Macromol. Chem. Phys.* 2005, *206*, 1472-1478.

[21] Lee, Y. R.; Raghu, A. V.; Jeong, H. M.; Kim, B. K. *Macromol. Chem. Phys.* 2009, *210*, 1247-1254.
[22] Kim, B. K.; Seo, J. W.; Jeong, H. M. *Eur. Polym. J.* 2003, *39*, 85-91.
[23] Jeong, H. M.; Lee, S. H. *J. Macromol. Sci., Phys.* 2003, *B42*, 1153-1167.
[24] Jeong, H. M.; Jang, K. H.; Cho, K. *J. Macromol. Sci., Phys.* 2003, *B42*, 1249-1263.
[25] Wang, D.; Choi, D.; Li, J.; Yang, Z.; Nie, Z.; Kou, R.; Hu, D.; Wang, C.; Saraf, L. V.; Zhang, J.; Aksay, I. A.; Liu, J. *ACS Nano* 2009, *3*, 907-914.
[26] Li, X.; Cai, W.; An, J.; Kim, S.; Nah, J.; Yang, D.; Piner, R.; Velamakanni, A.; Jung, I.; Tutuc, E.; Banerjee, S. K.; Colombo, L.; Ruoff, R. S. *Science* 2009, *324*, 1312-1314.
[27] Karmakar, S.; Kulkarni, N. V.; Nawale, A. B.; Lalla, N. P.; Mishra, R.; Sathe, V. G.; Bhoraskar, S. V.; Das, A. K. *J. Phys. D: Appl. Phys.* 2009, *42*, 115201/1-115201/14.
[28] Rollings, E.; Gweon, G. H.; Zhou, S. Y.; Mun, B. S.; McChesney, J. L.; Hussain, B. S.; Fedorov, A. V.; First, P. N.; de Heer, W. A.; Lanzara, A. *J. Phys. Chem. Solids* 2006, *67*, 2172-2177.
[29] Schniepp, H. C.; Li, J.-L.; McAllister, M. J.; Sai, H.; Herrera-Alonso, M.; Adamson, D. H.; Prud'homme, R. K.; Car, R.; Saville, D. A.; Aksay, I. A. *J. Phys. Chem. B* 2006, *110*, 8535-8539.
[30] McAllister, M. J.; Li, J.-L.; Adamson, D. H.; Schniepp, H. C.; Abdala, A. A.; Liu, J.; Herrera-Alonso, M.; Milius, D. L.; Car, R.; Prud'homme, R. K.; Aksay, I. A. *Chem. Mater.* 2007, *19*, 4396-4404.
[31] Kudin, K. N.; Ozbas, B.; Schniepp, H. C.; Prud'homme, R. K.; Aksay, I. A.; Car, R. *Nano Lett.* 2008, *8*, 36-41.
[32] Velasco-Santos, C.; Martinez-Hernandez, A. L.; Fisher, F. T.; Ruoff, R.; Castano, V. M. *Chem. Mater.* 2003, *15*, 4470-4475.
[33] Liu, N.; Luo, F.; Wu, H.; Liu, Y.; Zhang, C.; Chen, J. *Adv. Funct. Mater.* 2008, *18*, 1518-1525.
[34] Kim, H.; Macosko, C. W. *Polymer* 2009, *50*, 3797-3809.
[35] Ramanathan, T.; Abdala, A. A.; Stankovich, S.; Dikin, D. A.; Herrera-Alonso, M.; Piner, R. D.; Adamson, D. H.; Schniepp, H. C.; Chen, X.; Ruoff, R. S.; Nguyen, S. T.; Aksay, I. A.; Prud'Homme, R. K.; Brinson, L. C. *Nat. Nanotechnol.* 2008, *3*, 327-331.
[36] Jang, J. Y.; Kim, M. S.; Jeong, H. M.; Shin, C. M. *Compos. Sci. Technol.* 2009, *69*, 186-191.
[37] Jang, J. Y.; Jeong, H. M.; Kim, B. K. *Macromol. Res.* 2009, *17*, 626-629.
[38] Lee, H. B.; Raghu, A. V.; Yoon, K. S.; Jeong, H. M. *J. Macromol. Sci., Part B: Phys.* 2010, *49*, 802-809.
[39] Liu, J.; Yang, W.; Tao, L.; Li, D.; Boyer, C.; Davis, T. P. *J. Polym. Sci., Part A: Polym. Chem.* 2009, *48*, 425-433.
[40] Matsuo, Y.; Tahara, K.; Sugie, Y. *Carbon* 1996, *34*, 672-674.
[41] Matsuo, Y.; Tahara, K.; Sugie, Y. *Carbon* 1997, *35*, 113-120.
[42] Nguyen, D. A.; Lee, Y. R.; Raghu, A. V.; Jeong, H. M.; Shin, C. M.; Kim, B. K. *Polym. Int.* 2009, *58*, 412-417.
[43] Jeong, H. M. *Polym. Polym. Compos.* 2010, 18, 351-358.
[44] Raghu, A. V.; Lee, Y. R.; Jeong, H. M.; Shin, C. M. *Macromol. Chem. Phys.* 2008, *209*, 2487-2493.

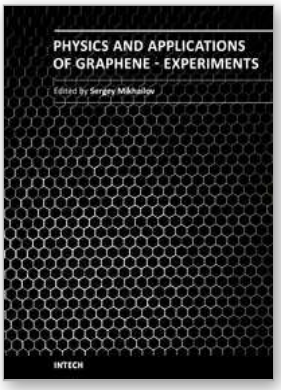

Physics and Applications of Graphene - Experiments

Edited by Dr. Sergey Mikhailov

ISBN 978-953-307-217-3
Hard cover, 540 pages
Publisher InTech
Published online 19, April, 2011
Published in print edition April, 2011

The Stone Age, the Bronze Age, the Iron Age... Every global epoch in the history of the mankind is characterized by materials used in it. In 2004 a new era in material science was opened: the era of graphene or, more generally, of two-dimensional materials. Graphene is the strongest and the most stretchable known material, it has the record thermal conductivity and the very high mobility of charge carriers. It demonstrates many interesting fundamental physical effects and promises a lot of applications, among which are conductive ink, terahertz transistors, ultrafast photodetectors and bendable touch screens. In 2010 Andre Geim and Konstantin Novoselov were awarded the Nobel Prize in Physics "for groundbreaking experiments regarding the two-dimensional material graphene". The two volumes Physics and Applications of Graphene - Experiments and Physics and Applications of Graphene - Theory contain a collection of research articles reporting on different aspects of experimental and theoretical studies of this new material.

INTECH
open science | open minds

InTech Europe
University Campus STeP Ri
Slavka Krautzeka 83/A
51000 Rijeka, Croatia
Phone: +385 (51) 770 447
Fax: +385 (51) 686 166
www.intechopen.com

InTech China
Unit 405, Office Block, Hotel Equatorial Shanghai
No.65, Yan An Road (West), Shanghai, 200040, China
中国上海市延安西路65号上海国际贵都大饭店办公楼405单元
Phone: +86-21-62489820
Fax: +86-21-62489821